

Neural Radiance Field (NeRF), capable of synthesizing high-quality novel viewpoint images, suffers from issues like artifact occurrence due to its fixed sampling points during rendering. This study proposes a method that optimizes sampling points to reduce artifacts and produce more detailed images.

1. Introduction

The diagram illustrates the proposed method's architecture. It starts with a **Camera** observing a 3D scene. A specific location is identified as the **Target pixel**. This pixel is processed by a **Sampling module**, which generates **Optimized sampling points**. These points are then fed into a **NeRF module** to produce the final **Predicted Per-pixel color**.

Rendering using NeRF involves estimating the color information and probability density at sample points along each ray, thereby estimating the expected color value for each pixel. A key consideration here is that the positions of these sampling points influence the quality of the images produced. Canonical NeRF places these points at regular intervals, regardless of the scene’s attributes, resulting in artifacts near thin or light objects.

The diagram illustrates the proposed feature fusion module. It takes 'Input features' (represented by four blue squares) as input. These features are fed into two parallel processing blocks: 'Ray-wise MLP' and 'Scene-wise MLP'. The outputs of these two MLPs are then combined in a 'Concat' step, represented by a sequence of eight colored squares (four green and four orange). Finally, the concatenated features are passed through a 'Linear' layer (a white rectangle) to produce the 'Output features' (represented by four light blue squares).

2. Related work

(a) Ray-wise MLP

(b) Scene-wise MLP

around the objects, as in the proposed method, has yet to be adequately investigated.

3.1 Key idea This study proposes a novel viewpoint image generation method using NeRF with optimized sampling points. The proposed method incorporates a MLP-Mixer-based architecture into NeRF module in a cascading manner, allowing simultaneous selection of optimal sampling points and NeRF training in an end-to-end manner. We anticipate the reduction of artifacts during rendering by concentrating sampling points primarily in critical areas, particularly object surfaces.

The sampling module's output serves as input for a con-

* Information Science and Biomedical Engineering Program,
Kagoshima University
Korimoto 1-21-40, Kagoshima, 890-0065 Japan

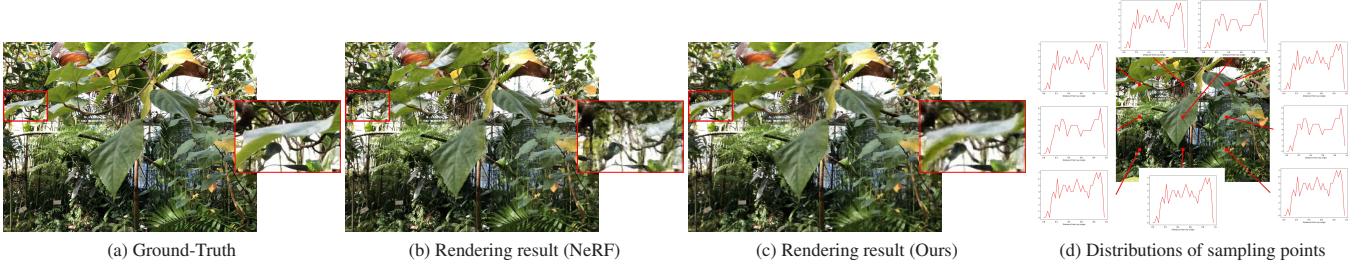


Fig. 4. Examples of rendered images for test view on Real Forward-Facing dataset.

Table 1. Results on Real Forward-Facing dataset.

		Room	Fern	Leaves	Fortress	Orchids	Flower	T-Rex	Horns	avg
PSNR	NeRF	31.79	24.99	20.83	31.06	20.39	27.43	26.19	26.97	26.82
	Ours	32.29	25.10	20.96	31.06	19.98	27.44	26.95	27.08	27.01
SSIM	NeRF	0.938	0.780	0.693	0.870	0.639	0.824	0.867	0.806	0.819
	Ours	0.943	0.790	0.707	0.878	0.623	0.827	0.884	0.813	0.824
LPIPS	NeRF	0.124	0.255	0.293	0.142	0.302	0.198	0.187	0.257	0.212
	Ours	0.111	0.243	0.278	0.153	0.312	0.196	0.168	0.243	0.204

ventional NeRF network. This NeRF module processes these inputs, including the estimated sampling points and direction vectors of camera rays as in the conventional NeRF, to estimate the color and density at those points. These calculated values are then used for volume rendering, leading to determining individual pixel colors and generating an image based on the given camera pose.

The model’s training process adheres to the conventional NeRF methodology.

3.3 Structure of the sampling module The sampling module G of the proposed method takes as input the camera center \mathbf{o} and the direction vectors \mathbf{d}_j (for $j \in \{1, \dots, N_r\}$) for N_r rays in the scene, and outputs the distances $t_{j,i}$ (for $i \in \{1, \dots, N_s\}$) from the origin to the sampling points i on the rays j . The sampling module G is structured with multiple layers of sampling blocks shown in Fig. 2, consisting of two integrated streams: a ray-wise MLP $G^{(ray)}$ for computing information along the camera rays and a scene-wise MLP $G^{(scene)}$ for calculating the information between the camera rays within the scene.

Ray-wise MLP $G^{(ray)}$ operates as a network that processes the features inherent to individual rays. Fig. 3(a) illustrates the architecture of $G^{(ray)}$. The MLP1 network comprises two fully connected layers, with the first layer’s output subjected to GELU activation function.

Scene-wise MLP $G^{(scene)}$ serves as a network that computes features based on the relationships among all rays within the scene, adopting a mechanism that allows consideration of the interrelations among feature vectors possessed by multiple rays. Fig. 3(b) shows the architecture of $G^{(scene)}$. The structure of MLP2 mirrors that of MLP1.

The features processed by the two MLPs are concatenated and subsequently refined by a linear layer to reduce them to the same dimension as the input. Finally, the sampling module yields distances of the sampling points $\{t_{j,i}\}$, converts them into 3D points $\mathbf{x}_{j,i}$, and then enters them into the NeRF module together with ray information \mathbf{d}_j .

4. Evaluation

Experiments were conducted on the real Forward-Facing dataset [1] to validate the effectiveness of adjusting sampling

point locations using the proposed method. We used one-eighth of the images from each scene as test images [1]. The training configuration for the proposed method’s network involved using 1,008 rays, i.e., $N_r = 1,008$, chosen randomly from $1,008 \times 756$ rays. Each ray had 128 sampling points, i.e., $N_s = 128$. The sampling module G implemented an MLP structure with three layers of the sampling blocks outlined in Fig. 2. The hidden layer of the ray-wise MLP $G^{(ray)}$ contains 1,024 units, while the scene-wise MLP $G^{(scene)}$ has 4,032 units in its hidden layer. Additionally, a Sigmoid function was incorporated into the output layer of G .

This experiment employed Peak Signal to Noise Ratio (PSNR), Structural Similarity (SSIM), and Learned Perceptual Image Patch Similarity (LPIPS) [5] as the benchmarks for assessing rendered image quality.

Table 1 shows the results for the eight scenes. Results are highlighted in bold, where significant differences were observed through the t-test with the significance level of 5%. Our method surpassed conventional NeRF in terms of PSNR, SSIM, and LPIPS in the Room, Fern, Leaves, and T-rex scenes.

Fig. 4 (a) to (c) demonstrate rendering examples from the test view. The results revealed that our method succeeded in rendering leaves that were not drawn by conventional NeRF.

The distribution of sampling points shown in Fig. 4(d) illustrates that sampling points tend to gather in areas thought to contain objects, contributing to the rendering of images with reduced artifacts.

5. Conclusions

This study introduces a learning-based method for optimizing sampling points in novel viewpoint image generation using NeRF. Our method adjusts the placement of sampling points based on scene properties, potentially reducing artifacts and enhancing image quality compared with conventional NeRF. Experiments with real images demonstrated the effectiveness of the proposed method in scene representation.

References

- (1) B. Mildenhall, et al. Nerf: Representing scenes as neural radiance fields for view synthesis. *Comm. ACM*, 65(1):99–106, 2021.
- (2) I. Tolstikhin, et al. Mip-mixer: An all-mlp architecture for vision. *Adv. Neural Inf. Process. Syst.*, 34:24261–24272, 2021.
- (3) J. T. Barron, et al. Mip-nerf: A multiscale representation for anti-aliasing neural radiance fields. *Int. Conf. Comput. Vis.*, pages 5855–5864, 2021.
- (4) A. Kurz, et al. Adanerf: Adaptive sampling for real-time rendering of neural radiance fields. *Eur. Conf. Comput. Vis.*, pages 254–270. Springer, 2022.
- (5) R. Zhang, et al. The unreasonable effectiveness of deep features as a perceptual metric. *Comput. Vis. Pattern Recognit.*, pages 586–595, 2018.